

# Journal of Basics and Applied Sciences Research (JOBASR) ISSN (print): 3026-9091, ISSN (online): 1597-9962

Volume 3(6) November 2025





## In Silico Evaluation and ADMET Profiling of Phytochemicals from *Diodia sarmentosa* as Potential Anti-Fibroid Agents.



Okoro C. A.<sup>1\*</sup>, Ezejiofor T.I.N.<sup>2</sup>, Mgbemena I.C.<sup>3</sup> & Ezeji E.U.<sup>4</sup>
<sup>1,2,3&4</sup>Department of Biotechnology, Federal University of Technology, Owerri-West L.G.A, 460114, Imo State, Nigeria

\*Corresponding Author Email: <a href="mailto:chiedu.okoro@gmail.com">chiedu.okoro@gmail.com</a>

### **ABSTRACT**

Uterine fibroids remain the most common benign gynecological tumours and a major cause of infertility among females of reproductive age. Diodia sarmentosa (DS) is traditionally used in African ethnomedicine for the treatment of uterine fibroids, with experimental studies validating its anti-fibroid effects in animal models. However, its bioactive compounds and molecular mechanisms remain poorly understood. Fourteen phytoconstituents were identified from DS extract using HPLC-UV. The phytochemical structures were retrieved from PubChem, while target proteins: progesterone, estrogen, and gonadotropin-releasing hormone 1 (GnRH1) receptors were obtained from the Protein Data Bank. Molecular docking was performed using PyRx. Control ligands included ulipristal acetate, estradiol, and elagolix for the progesterone, estrogen, and GnRH1 receptors, respectively. Post-docking analyses were performed using PyMol and Biovia Discovery Studio, and ADMET profiling via SwissADME and DataWarrior. Among twelve identified hits, quercetin (-8.7 kcal/mol), spirostanol (-8.0 kcal/mol), and 7-hydroxycoumarin (-6.9 kcal/mol) showed the strongest binding affinities for the progesterone, GnRH1, and estrogen receptors, respectively. Several phytochemicals demonstrated dual targeting of progesterone and estrogen receptors, while spirostanol uniquely interacted with both GnRH1 and estrogen receptors. These dual-target interactions suggest possible synergistic mechanisms among the phytochemicals, potentially underlying the traditional efficacy of DS in fibroid management. In silico ADMET profiling identified spirostanol with pharmacokinetic and safety properties comparable to the standard drug ulipristal acetate. This study provides scientific support for the ethnomedicinal use of DS and highlights its phytochemicals as promising scaffolds for potential anti-fibroid drug development, warranting further optimization and experimental validation for oral therapeutic application.

### **Keywords:**

Diodia sarmentosa, Uterine fibroids, Molecular docking, ADMET, Phytochemicals

### INTRODUCTION

Uterine fibroids (leiomyomas) are hormone-dependent histologically benign smooth muscle tumours of the uterus that affect up to 70–80% of adult women (Baird *et al* 2003; Ishikawa *et al*, 2009). Women of African descent are at increased risk of developing multiple and larger leiomyomata at younger ages than their white counterparts (Lewis et al. 2018). They persist as the most frequently occurring benign tumours in gynecology and are among leading causes of abnormal uterine bleeding, pelvic pain, and infertility (Zhang et al. 2025). Despite their high prevalence, management options for uterine fibroids remain limited. Minimally invasive approaches such as uterine artery embolization,

high-intensity MRI-guided focused ultrasound, laparoscopic or transcervical radiofrequency ablation, and pharmacological agents including ulipristal acetate or oral gonadotropin-releasing hormone antagonists with add-back therapy are available (De Smith et al 2025). definitive surgical treatments However, hysterectomy and myomectomy, while effective, are invasive, and medical therapies are constrained by concerns regarding safety and tolerability (De Smith et al 2025).

Pharmacotherapy has focused on modulating ovarian steroid hormones, given the estrogen- and progesterone-dependence of fibroid growth (Lewis et al. 2018). Gonadotropin-releasing hormone (GnRH) agonists and

antagonists reduce fibroid volume but are associated with hypoestrogenic side effects (e.g., bone loss, vasomotor symptoms) (Lewis et al. 2018). Selective progesterone receptor modulators (SPRMs) such as ulipristal acetate have demonstrated clinical efficacy in controlling heavy menstrual bleeding and reducing fibroid volume by inducing apoptosis and downregulating proliferation in fibroid tissue. Ulipristal acetate is FDA-approved for emergency contraception and was approved in Europe for fibroid management; however, concerns about rare cases of liver toxicity led to regulatory restrictions, underscoring the need for safer alternatives.

Natural products represent valuable reservoirs for novel drug discovery, with phytochemicals offering structural diversity and potential multi-target effects relevant to complex health challenges such as uterine fibroids. D. sarmentosa, (DS) a medicinal plant used traditionally in African ethnomedicine, for the treatment of injuries, edema, diarrhea, dysentery, and skin infections (Elechi et al., 2020; Anyanwu-Azuka et al., 2022). In South East Nigeria, DS extract has been used traditionally in treating uterine fibroids in women. Scientific studies underscore the traditional uses of DS. Several studies have confirmed the presence of bioactive components such as flavonoids, phenols, saponins, alkaloids, terpenoids and tannins with reported antioxidant and anti-proliferative properties (Elechi et al., 2020; Okoroafor et al., 2020; Ezejiofor & Okorafor, 2022; Sani et al., 2025). Its anti-ulcer potential (Akah et al., 1998), anti-inflammatory and analgesic effects (Umoh et al. 2016) have been reported by several studies. Ezejiofor and Okorafor (2022) reported the antiuterine fibroid efficacy of DS ethanol leaves extract in monosodium glutamate induced uterine fibroid in female albino rats. In another study, ethanol leaves extract of DS was effective against diethyl nitrosamine-induced hepatocellular carcinoma in albino rats (Ezejiofor & Okoroafor, 2019).

Although DS has long been used in traditional medicine ailments including uterine tumours. phytochemicals have never been investigated within the framework of modern drug discovery. In particular, the identification of its bioactive phytoconstituents, their drug-likeness and pharmacokinetic suitability for oral fibroid therapy remain uncharacterized. To address this gap, this research provided preliminary in-silico drug discovery assessment of DS phytochemicals using molecular docking, post docking analysis and ADMET characterization of DS. In-silico methods provide a rapid and cost-effective platform for integrating receptor binding with pharmacokinetic and safety assessments, enabling rational prioritization of compounds before experimental validation and supporting the identification of orally bioavailable, safe, and pharmacologically relevant candidates for uterine fibroid therapy (Lipinski et al., 2001; Veber et al., 2002).

## MATERIALS AND METHODS

Plant materials harvesting and identification: Fresh samples of DS aerial parts were collected from Obinze Village, Owerri West Local Government Area, Imo State, Nigeria. The plant specimen was accurately identified and authenticated by a plant taxonomist in the Department of Biology, Federal University of Technology, Owerri. The identification was confirmed with a Kew Herbarium reference number: K006212000 (http://specimens.kew.org/herbarium/K006212000).

Plant Extracts Preparation and Extraction: Fresh DS aerial parts were sorted, washed with water followed with distilled water and air dried to constant weight at room temperature for about 2-4 weeks. The dried plant materials were ground into fine powder using an electric grinding machine. Extraction was carried out by maceration as described by Erhirhie and Ilodigwe (2019). The resulting crude extracts were weighed and stored in air tight opaque containers for HPLC- UV analysis.

High performance liquid chromatography analysis: The 70% ethanol extracts were analyzed using HPLC-UV (Shimadzu, Nexera MX, HPLC system), equipped with a UV- Diode Array Detector (DAD) detector. The equipment is fitted with UBondapak C18 column with a length of 100mm, internal diameter of 4.6mm and  $7\mu m$  thickness.

Hardware, softwares and webserver databases: A computer system: ASUS VivoBook laptop. Operating system: Windows 11 Pro. Processor: Intel(R) Core (TM) i5-7200U CPU @ 2.50GHz, 2.71 GHz processor, 8.00 GB RAM. Free web servers: PubChem database, Protein Data bank (PDB) database and Swiss ADME. Softwares: Open Babel software (Version 2.4.1), PyRx software (Version 0.8), Pymol software (25.1.0), Data Warrior software (Version 06.1.0) and Discovery studio software.

**Preparation of Ligands:** The HPLC-UV identified phytochemicals from DS and co-crystallized control ligands: estradiol, ulipristal acetate and elagolix were downloaded from <a href="https://pubchem.ncbi.nlm.nih.gov">https://pubchem.ncbi.nlm.nih.gov</a> in SDF format. The ligands were concatenated with Open Babel software for easier docking process.

**Preparation of Targets:** X-ray diffraction 3D structures of three uterine fibroid targets namely estrogen receptor, gonadotropin releasing hormone 1 receptor (GnRH1R) and progesterone receptor with PDB IDs 5TOA, 7BR3 and 1E3K respectively were downloaded in PDB format from <a href="https://www.rcsb.org">https://www.rcsb.org</a>. The 3D structures of the target proteins were prepared for docking using PyMol software and saved in PDB format.

Molecular docking and post docking analysis: Energy minimization of ligands was performed using the universal force field (UFF) protocol in the PyRx software. The steepest descent algorithm was applied to ensure that all ligands had the lowest possible energy states before docking. Similarly, the ligands were converted to PDBQT format using the PyRx software prior to the docking process. Molecular docking process was executed with PyRx software.

Post docking analysis involved viewing each ligandprotein complex (preserved in PDB format via PyRx) in PyMol. Biovia Discovery Studio software was used to view and analyze the binding site interactions involving the targets, ligands and the amino acid residues in 2D and 3D.

In-silico ADMET analysis: The basic physicochemical, lipophilicity, water solubility parameters, bioavailability radar plot, drug likeness, pharmacokinetics parameters such as Absorption, Distribution, Metabolism, and Excretion and medicinal chemistry predictions were evaluated for each ligand using SwissADME, an online tool from the Swiss Institute of Bioinformatics (http://www.swissadme.ch/index. php) (Mendie & Hemalatha, 2022; Jha, 2023). The in-silico toxicity prediction was carried out with DataWarrior software (www.open

molecules.org). The software also predicted potential toxicological risks, including mutagenicity, tumorigenicity, reproductive toxicity, and irritability, using in-built models and toxicological databases (Shivakumar et al., 2018).

### RESULTS AND DISCUSSION

HPLC Identified Phytochemicals in DS Extract: In Fig 1, HPLC-UV analysis of DS identified fourteen distinct peaks representing different chemical compounds, thereby highlighting the broad chemical diversity within the sample. The identified phytochemicals are benzoic acid, gallic acid, resveratrol, dihydroguaiaretic acid, 3-pentadecyl-phenol, squalene, quercetin, kaempferol, rutin, isoquercitrin, quercitrin, 7-hydroxycoumarin, astragalin and spirostanol. The retention times ranged between 1.300 and 14.333, the peak area values varied between 30.4350 and 206.4160, while the peak height ranged between 1.939 and 15.689. All probable compounds identified by HPLC-UV screening in this study were used as ligands in molecular docking to establish their potential anti-fibroid properties.

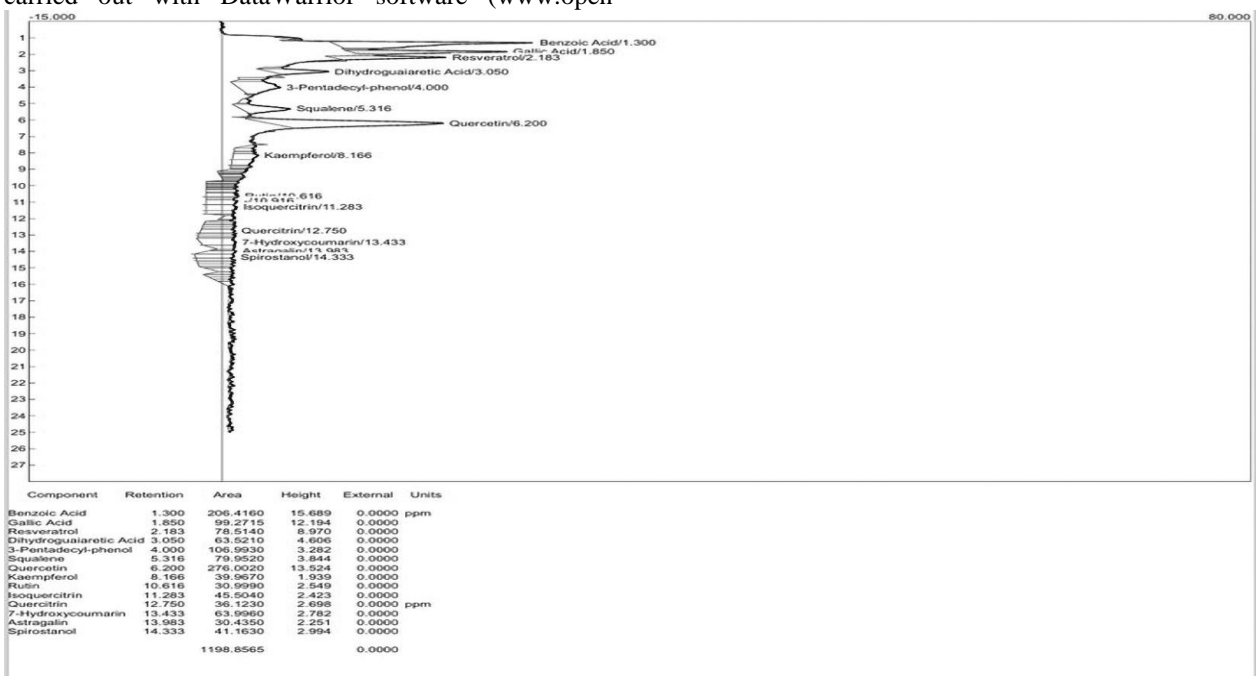


Fig 1: HPLC chromatogram of *Diodia sarmentosa* extract

Molecular Docking Results for Identified Phytochemicals: Molecular docking provides a rational framework for predicting ligand - receptor interactions by estimating the binding free energy and identifying key

bonds that stabilize the ligand-protein complex (Dar & Mir, 2017; Iheagwam, et al., 2019). In the present study, docking analyses were conducted against three therapeutically relevant targets: estrogen receptor (ER; PDB ID: 5TOA), gonadotropin-releasing hormone 1

receptor (GnRH1R; PDB ID: 7BR3), and progesterone receptor (PR: PDB ID: 1E3K) using estradiol, elagolix. and ulipristal acetate (-6.0, -7.0, and -6.7 kcal/mol, respectively) as reference ligands. The obtained results are generally consistent with previously reported docking scores for estrogen receptor-α (-6.6 kcal/mol) (Roy et al., 2024). However, they differ from the reported values for GnRH1R (-11 kcal/mol) (Li et al., 2022), likely due to the use of a different docking software suite, and for the progesterone receptor (-8.21 kcal/mol) (Rajamiriyam et al., 2022). Estradiol, elagolix, and ulipristal acetate were used as control ligands because they are clinically established modulators of estrogen, GnRH1, and progesterone receptors respectively, making them key molecular targets in uterine fibroid pathophysiology. Their co-crystallized structures from the protein data bank (PDB) provided validated reference templates for benchmarking docking accuracy and comparing the binding affinities of test phytochemicals. The selected targets have been used as targets of interest in other similar studies (Rama et al., 2022; Ciceri, et al., 2024; Dourado et al., 2025).

Compounds exhibiting binding affinities equal to or more favourable than these benchmarks were prioritized for further evaluation. Except for benzoic acid and gallic acid, all screened phytochemicals displayed valid interactions with at least one receptor target. Among the top-performing ligands, 7-hydroxycoumarin (-6.9 kcal/mol) demonstrated the strongest affinity for ER. Spirostanol (-8.0 kcal/mol) had the most potent binding affinity with GnRH1R, and quercetin (-8.7 kcal/mol) exhibited the highest binding affinity for PR. Notably in Table 1, ten compounds displayed dual-target activity, suggesting potential poly pharmacological properties (Kaushik, et al., 2025). Molecular docking simulations revealed distinct binding modes for the selected ligands, with stabilization mediated by a variety of non-covalent interactions. The ligands engaged key active-site residues through conventional hydrogen bonds, alkyl and carbonhydrogen contacts, pi-alkyl, pi-sigma, pi-anion, and pi-pi T-shaped interactions, as well as occasional unfavorable donor-donor or acceptor-acceptor contacts as presented in Table 1. The two-dimensional interaction diagrams of the hit compounds with the three targets are presented in Figure 2. The formation of conventional hydrogen bonds with key active-site residues is a feature known to enhance binding affinity by displacing protein-bound water molecules and to contribute critically to ligandreceptor specificity. Several ligands interacted with their respective receptors forming conventional hydrogen bonds as presented in Table 1. In contrast, 7hydroxycoumarin, squalene, and 3-pentadecyl-phenol bound to ER; 7-hydroxycoumarin, spirostanol, and 3pentadecyl-phenol bound to the GnRH1 receptor; and squalene and benzoic acid bound to PR, all without conventional hydrogen-bonding interactions. Ligands

that did not form conventional hydrogen bonds with active-site residues also engage in stable binding via hydrophobic, pi-pi, van der Waals, or other non-polar interactions, particularly within lipophilic pockets of the orthosteric site (De Freitas & Schapira, 2017; Patil et al. 2010). Moreover, absence of hydrogen-bond interactions with known active site residues could also indicate binding at allosteric or secondary sites, which can modulate receptor activity via conformational changes, as shown in dual-site inhibitors designs (Huang et al. 2021). In Table 1, molecular docking simulations demonstrated diverse interactions stabilizing the phytochemicalreceptor complexes. Spirostanol exhibited strong hydrophobic stabilization with the GnRH1 receptor through alkyl interactions involving Leu238, Lys267, Val270, and Ala271, while its binding to PR was characterized by alkyl and pi-alkyl bonds with Phe 818, Val 729, Pro 696, Trp 765, His 770, and Arg 766, along with a hydrogen bond to Arg766. 3-pentadecyl-phenol formed a hydrogen bond with Leu715, extensive alkyl interactions with Met 756, Leu 887, Leu 718, Leu 721, Met 759, Met 801, Val 760, Leu 763, and Leu 797, and pi-alkyl contacts with Leu 715, Cys 891, Phe 778, and Phe 794. 7-hydroxycoumarin interacted with Gln725 via hydrogen bonding, pi-sulfur contact with Met759, pi-pi T-shaped interaction with Phe778, pi-alkyl contact with Leu718, and an unfavorable donor-donor interaction with Arg766. Astragalin engaged Trp765 (hydrogen bond), Met759 (pi-sulfur), Gln815 (unfavorable donor-donor), Val698 (pi-sigma), Pro696 (pi-alkyl), Arg766 (pi-cation), and Glu695/Asp697 (pi-anion). Isoquercitrin formed hydrogen bonds with His770, Val698, Pro696, and Arg766, together with pi-cation (Arg766), pi-anion (Glu695), and pi-alkyl contacts (Pro696, Arg766). Kaempferol interacted through a hydrogen bond with Val698, pi-cation contacts with Arg766 and Lys822, pianion with Glu695, and pi-alkyl contacts with Pro698 and Arg766. Quercetin bound via a hydrogen bond to Gln 725, alkyl contacts with Pro 696, Arg 766, Val 729, Leu 758, and Met 759, pi-alkyl with Trp 765, Pro 696, and Val 729, and an unfavorable donor-donor contact with Lys 822. Quercitrin formed hydrogen bonds with Gln 815, His 770, and Ile 699, a carbon-hydrogen bond with Val698, pi-cation (Arg766), pi-pi T-shaped (Trp 765), and pi-alkyl (Pro 696) interactions. Resveratrol engaged (hydrogen bond), Arg766 (donor-donor), Leu715 Met759 (pi-sulfur), Phe778 (pi-pi T-shaped), and Leu718/Leu763 (pi-alkyl). Rutin formed hydrogen bonds with Gln725 and Gln815, a carbon-hydrogen bond with Lys822, pi-cation (Arg766), pi-donor hydrogen (Ile 699), pi-sigma (Val698), amide-pi stacked (Asp 697), alkyl (Arg 766, Lys 769), and multiple pi-alkyl contacts with Trp765, His 770, Val 698, Ile 699, Arg 766, and Ala 779. Dihydroguaiaretic acid bound through hydrogen bonds with Gln 725 and Ile 699, pi-cation (Arg 766), alkyl (Arg

766, Pro 696, Ile 699, Val 729, Leu 758, Lys822), and pialkyl contacts with Trp732, Trp765, Phe818, and Ile699. For the estrogen receptor, 3-pentadecyl-phenol exhibited pi-cation (His467), pi-anion (Glu337), pi-pi stacked (His467), alkyl (Ile404), and pi-alkyl (His464, His467) interactions. 7-hydroxycoumarin displayed a carbonhydrogen bond with Ser469, pi-anion (Glu337), pi-pi stacking (His467), and an unfavorable donor-donor contact with His467. Astragalin formed hydrogen bonds with Asp489, Tyr488, Glu375, and Lys471, together with pi-cation (His467), pi-sulfur (Met473), pi-pi T-shaped (His467), pi-alkyl (Pro412), and unfavorable donordonor (Glu337, Glu335) interactions. Dihydroguaiaretic acid exhibited hydrogen (Ser463) and carbon-hydrogen (Leu462) bonds, pi-cation (His467), pi-anion (Glu337), pi-pi stacked (His467), alkyl (Met410, Met473), and pialkyl (His467) bonds. Kaempferol bound via hydrogen bonds with Glu332 and Ser463, pi-anion (Glu337),

sulfur-X (Met473), and pi-pi stacked (His467) interactions. Ouercetin established hydrogen bonds with Lys471, His467, Asp489, and Glu332, a carbonhydrogen bond with Ser409, a pi-anion interaction with Glu332, and an unfavorable donor-donor interaction with Tyr411. Quercitrin exhibited hydrogen bonds with Ser333, Glu332, and Met410, a pi-cation (Lys471), pisulfur (Met473), and alkyl (Pro412) bonds. Resveratrol was stabilized by a pi-anion (Glu337) and pi-pi stacked (His467) interaction. Rutin formed hydrogen bonds with Ser333, Glu332, and Ser408, a carbon-hydrogen bond with Ser333, an unfavorable donor-donor (Met410), a pisulfur (Met473), and pi-alkyl (His467) bonds. Squalene binding was dominated by a pi-sigma interaction with His467, an alkyl bond with Met473, and multiple pi-alkyl interactions involving His467, Trp335, His464, and Tvr488.

Table 1: Molecular docking and binding site interaction analysis result for DS extract phytochemicals

Phyto-compound	Pub chem	ER	ER binding	GnRH1R	GnRH1R	PR	PR binding site
	ID	Binding	site	Binding	binding site	Binding	interactions
		Affinity	interactions	Affinity	interactions	Affinity	
		(Kcal/mol)		(Kcal/mol)		(Kcal/mol)	
Benzoic acid	243	-5.3	H-bond: His 467, Lys 471, Glu337, met 341, ASN 470; C-H- bond: His 467; Pi Anion: Glu 337; Pi sulfur: Met 410; Pi-Pi stacked: His 467; Pi Alkyl: His 467	-4.4	H-bond: Arg 240; C-H- bond: Gly1145; Pi- Pi stacked: Phe 236	-5.9	Pi-sigma: Met 759; Pi-pi T- shaped: Phe 778; Pi-alkyl: Leu 763; Unfavourable donor-donor: Arg 766
Gallic acid	370	-4.1	H-bond: His 467, Glu 337, Leu 462, Ser 408; Pi-Pi stacked: His 467; Pi anion: Glu 337	-3.2	H-bond: Thr 274, Thr 277; Pi-Sigma: Leu 228	-4.4	H-bond: Gln 725, Arg 766; Pi-Pi Tshaped: Phe 778; Pi Alkyl: Leu 718; Unfavourable acceptor- aceptor: Met 759
3-Pentadecyl- phenol	68146	-6.7	Pi-cation: His467; Pi- anion: Glu337; Pi- Pi stacked: His467; Alkyl: Ile404; Pi-alkyl:	-4.5	Alkyl: Lys267, Val 270, Ile 235, Leu 238, Leu 242; Pi-alkyl: Phe 326, Val 270, Ala 271	-7.3	H-bond: Leu715; Alkyl: Met756, Leu887, Leu718, Leu721, Met759, Met801,

Resveratrol	445154	-6.3	His464, His467  Pi-anion: Glu337; Pi– Pi stacked: His467	-5.8	H-bond: Thr 237, Arg 240; Pi-Pi stacked: Phe 236	-8.3	Val760, Leu763, Leu797; Pi- alkyl: Leu715, Cys891, Phe778, Phe794 H-bond: Leu715; Donor-donor: Arg766; Pi- sulfur: Met759; Pi-Pi T-shaped:
Dihydroguaiaretic	476856	-6.1	H-bond:	-5.8	H-bond: Thr	-7.7	Phe778; Pi- alkyl: Leu718, Leu763 H-bonds:
Acid	470030	-0.1	Ser463; C–H: Leu462; Pi- cation: His467; Pi- anion: Glu337; Pi- Pi stacked: His467; Alkyl: Met410, Met473; Pi- alkyl: His467	-3.0	239, Ile 235, Ala 273, Pi- sigma: Val 278; Alkyl: Val 270, Val 278; Pi Alkyl: Val 270, Ala 273	-77	Gln725, Ile699; Pi- cation: Arg766; Alkyl: Arg766, Pro696, Ile699, Val729, Leu758, Lys822; Pi- alkyl: Trp732, Trp765, Phe818, Ile699
Squalene	638072	-6.3	Pi-sigma: His467; Alkyl: Met473; Pi- alkyl: His467, Trp335, His464, Tyr488	-5.1	Pi-Alkyl: Phe 236; Alkyl: Leu 238, Val 270, Ala 271, Ile 235, Leu 238, Leu 242	-4.9	Pi-alkyl: Met 759, Val 729, Ile 699, Pro 696, Arg 766, Phe 818, Lys 769, Trp 765, His 770, Met 692, Val 698
Quercetin	5280343	-6.6	H-bonds: Lys471, His467, Asp489, Glu332; C– H: Ser409; Pi-anion: Glu332; Unfavourable donor–donor: Tyr411	-6.3	H-bond: Arg 240, Thr 237, Pro 1123; Pi- Pi stacked: Phe 236	-8.7	H-bond: Gln725; Alkyl: Pro696, Arg766, Val729, Leu758, Met759; Pi- alkyl: Trp765, Pro696, Val729; Unfavourable donor—donor: Lys822
Quercitrin	5280459	-6.7	H-bonds: Ser 333, Glu 332, Met 410; Pi- cation: Lys471; Pi-	-6.8	H-bond: Ser 140, Thr 144, Arg 240, Ile 143; Pi- Alkyl: Lys	-7.6	H-bonds: Gln815, His770, Ile699; C–H: Val698; Pi-cation:

Isoquercitrin	5280804	-5.8	sulfur: Met473; Alkyl: Pro 412 H-bond: Glu 337, Ser 408, Ser 469, Asn, 470; Pi- Sigma: Met 379; C-H- bond: Ser 330; Pi- Anion: Glu 375; Pi- Cation: His 467; Pi-Pi Static: His	-6.6	233; Pi-Pi stacked: Phe 236  H-bond: Thr 144, Lys 233, Thr 237; Pi- sigma: Lys 233; Amide Pi-stacked: Ala 232; Pi- Alkyl: Lys 233	-7.6	Arg766; Pi–Pi T-shaped: Trp765; Pi- alkyl: Pro696 H-bonds: His770, Val698, Pro696, Arg766; Pi- cation: Arg766; Pi- anion: Glu695; Pi-alkyl: Pro696, Arg766
Rutin	5280805	-6.2	H-bonds: Ser333, Glu332, Ser408; C-H: Ser333; Pi- sulfur: Met473; Pi- alkyl: His467; Unfavourable donor-donor: Met410	-6.9	H-bond: Arg 240, Ile 229; Unfavourable donor-donor: Arg 240; Pi- Pi stacked: Phe 236; Pi- Alkyl: Lys 233, Ala 232	-7.6	H-bonds: Gln725, Gln815; C-H: Lys822; Pi- cation: Arg766; Pi- donor H-bond: Ile699; Pi- sigma: Val698; Amide-pi stacked: Asp697; Alkyl: Arg766, Lys769; Pi- alkyl: Trp765, His770, Val698, Ile699, Arg766, Ala779
Kaempferol	5280863	-6.3	H-bonds: Glu332, Ser463; Pi- anion: Glu337; Sulfur–X: Met473; Pi– Pi stacked: His467	-6.2	H-bond: Arg 240; Pi-Pi stacked: Phe 236; Pi Alkyl: Lys 233	-7.8	H-bond: Val698; Pi- cation: Arg766, Lys822; Pi- anion: Glu695; Pi-alkyl: Pro698, Arg766
7- Hydroxycoumarin	5281426	-6.9	C–H: Ser469; Pi-anion: Glu337; Pi– Pi stacked: His467; Unfavourable donor–donor: His467	-5.2	H-bond: Arg 240; Pi-Pi stacked: Phe 236; Pi- Alkyl: Ly 233	-6.8	H-bond: Gln725; Pi- sulfur: Met759; Unfavourable donor-donor: Arg766; Pi-Pi T-shaped:

Astragalin	5282102	-6.1	H-bonds: Asp489, Tyr488, Glu375, Lys471; Pi- cation: His467; Pi- sulfur: Met473; Pi- Pi T-shaped: His467; Pi- alkyl: Pro412; Unfavourable donor—donor: Glu337, Glu335	-6.6	H-bond: Phe 1195; Unfavourable acceptor-acceptor: Ile 143; Pication: Arg 240; Pi-Alkyl: Lys 233; Pi-Pistacked: Phe 236; Pi-Pi T shaped; Phe 1195	-7.4	Phe778; Pi-alkyl: Leu718 H-bond: Trp765; Pi-sulfur: Met759; Unfavourable donor–donor: Gln815; Pi-sigma: Val698; Pi-alkyl: Pro696; Pi-cation: Arg766; Pi-anion: Glu695, Asp697
Spirostanol	12304444	-0.6	H-bond: Ser 469; Alkyl: Met 473; Pi Alkyl: Trp 335, His: 467	-8.0	Alkyl: Leu238, Lys267, Val270, Ala271	-8.3	H-bond: Arg766; Alkyl: Arg766, Pro696, Val729; Pi- Alkyl: Phe818, Trp765, His770,
Control		-6.0		-7.0		-6.7	

<sup>5</sup>TOA- estradiol receptor, 7BR3 – gonadotropin releasing hormone 1,1E3K – progesterone receptor

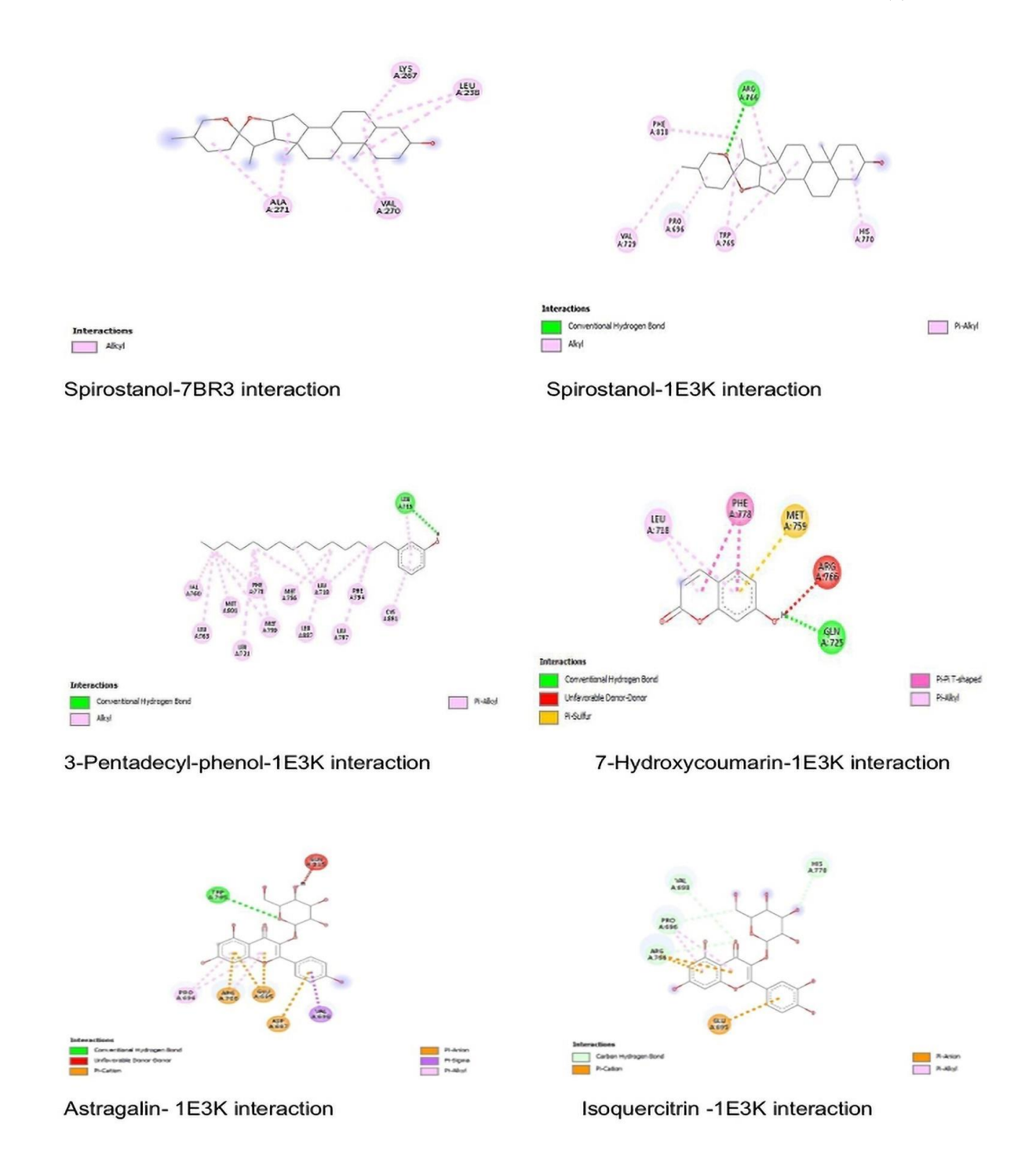


Fig 2A: 2D binding site interactions of D. sarmentosa hits with GnRH1 (7BR3) and progesterone (1E3K) receptors

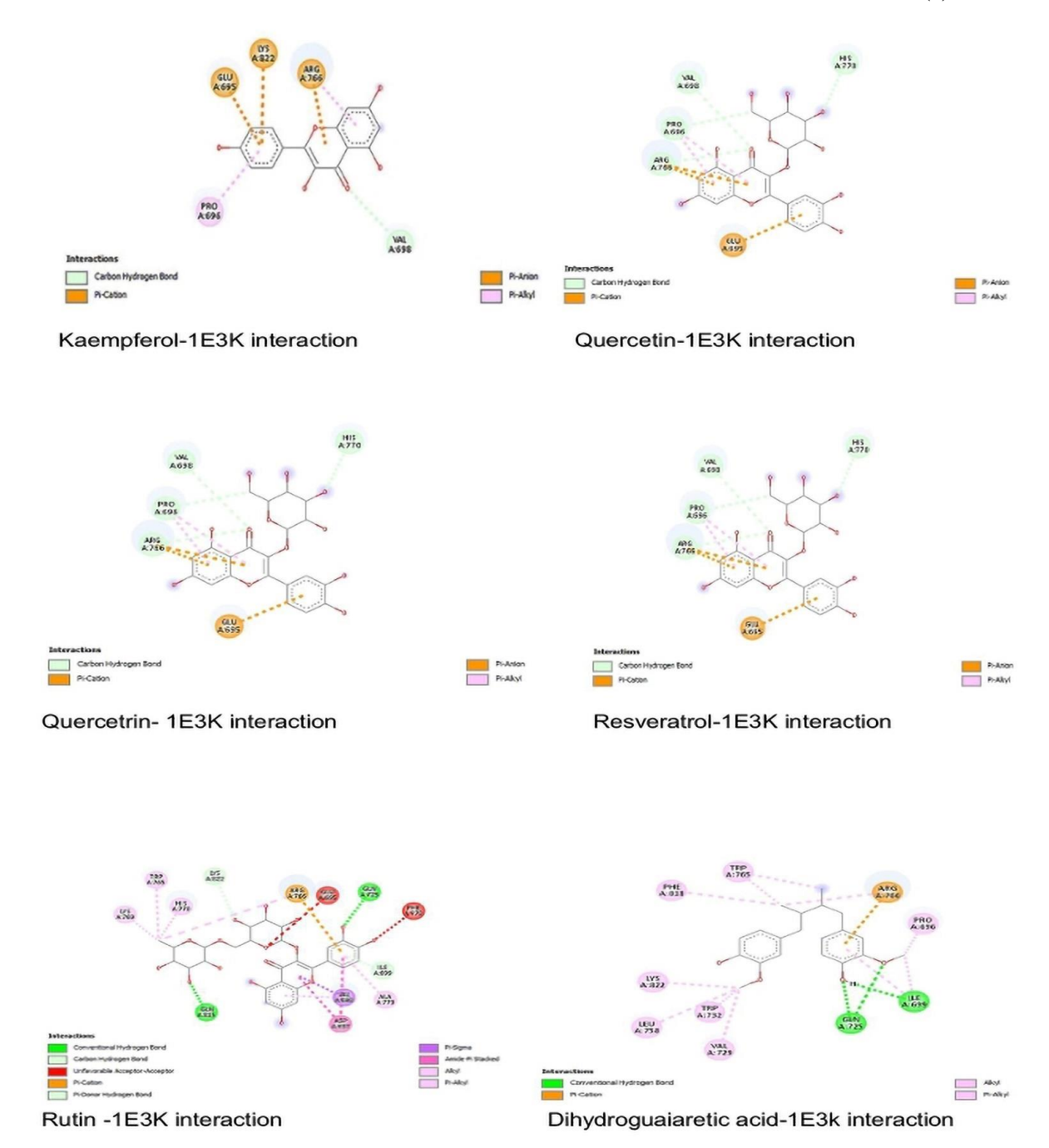


Fig 2B: 2D binding site interactions of *D. sarmentosa* hits with progesterone receptor (1E3K)

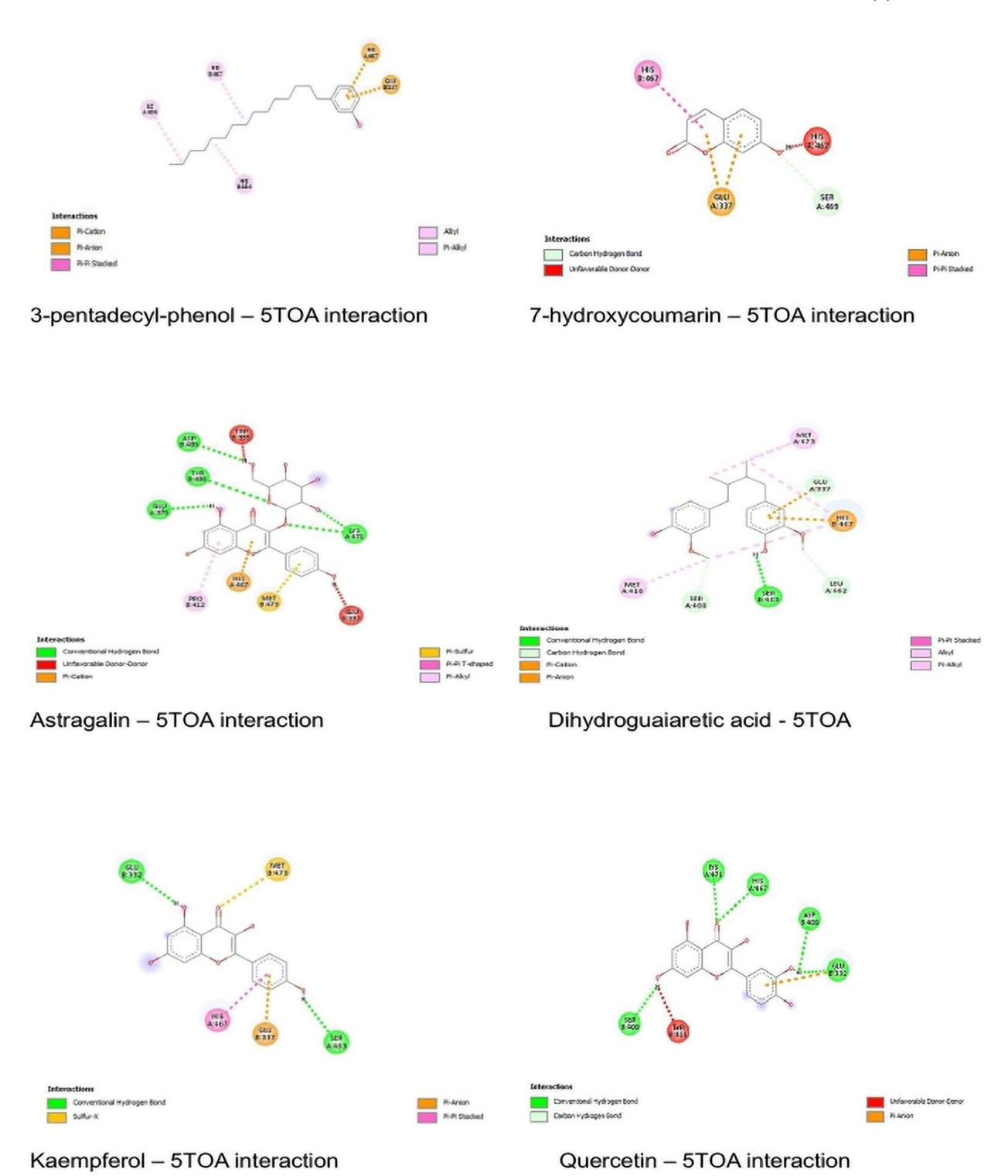
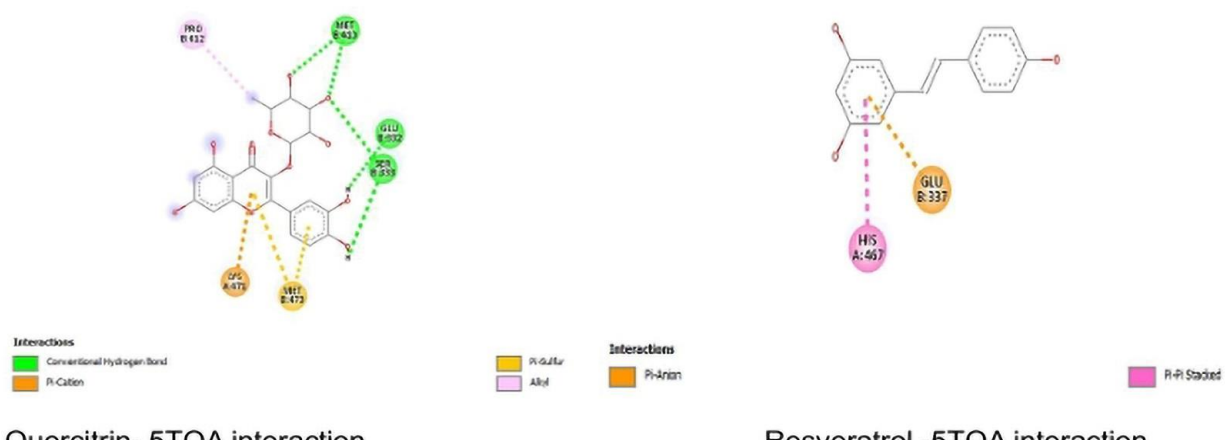
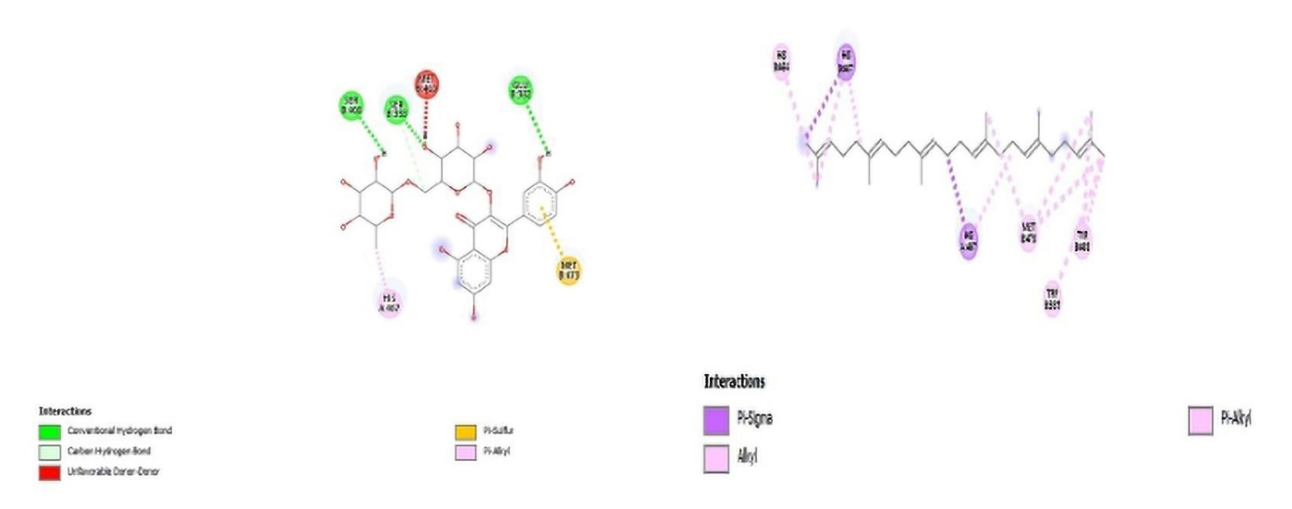


Fig 2C: 2D binding site interactions of *D. sarmentosa* hits with estrogen receptor (5TOA)



Quercitrin- 5TOA interaction

Resveratrol -5TOA interaction



Rutin - 5TOA interaction

Squalene - 5TOA interaction

Fig 2D: 2D binding site interactions of D. sarmentosa hits with estrogen receptor (5TOA) (continued) Toxicity Screening of Identified DS Extract **Phytochemicals:** In silico toxicity prediction is a crucial aspect of modern drug discovery, allowing early detection of compounds with potential safety risks. Toxicity prediction tools estimate acute, organ-specific, genotoxic, and carcinogenic effects by identifying structural features linked to toxicity. This approach also reduces animal testing and directs experimental efforts on safer candidates for preclinical studies (Noga et al., 2024).

Toxicity predictions of the screened phytochemicals were performed using Data Warrior software as displayed in Table 2. The toxicity profiling revealed clear differences in the safety predictions of the tested phytochemicals. Out of the twelve hit compounds, eight compounds (3pentadecyl-phenol, dihydroguaiaretic acid, squalene,

quercitrin, isoquercitrin, rutin, astragalin, and spirostanol) were predicted to be non-toxic across all investigated parameters, indicating a favourable safety profile for further consideration in drug development. Resveratrol, quercetin, kaempferol, and 7-hydroxycoumarin displayed one or more toxicity risks, including mutagenicity, tumorigenicity, reproductive toxicity, or irritancy. Quercetin was the only compound predicted to be both mutagenic and tumorigenic, while resveratrol showed reproductive toxicity in addition to potential mutagenicity. Notably, ulipristal acetate, a standard drug was predicted to have potential reproductive toxicity. This finding may align with Mozzanega (2021) findings, who reported that ulipristal acetate is associated with liver failure. This toxicity prediction result suggest that the eight non-toxic compounds represent the most promising candidates for further pharmacological evaluation, whereas those flagged with potential toxic risks may require structural confirmation and optimization, formulation strategies, or careful dose-dependent safety assessments.

Table 2: Toxicity Screening Result for DS Phytochemicals

Compound name	Pubchem ID	Mutagenic	Tumorigenic	Reproductive Effective	Irritant
3-Pentadecyl-phenol	68146	None	None	None	None
Resveratrol	445154	High	None	High	None
Dihydroguaiaretic Acid	476856	None	None	None	None
Squalene	638072	None	None	None	None
Quercetin	5280343	High	High	None	None
Quercitrin	5280459	None	None	None	None
Isoquercitrin	5280804	None	None	None	None
Rutin	5280805	None	None	None	None
Kaempferol	5280863	High	None	None	None
7-Hydroxycoumarin	5281426	High	None	None	None
Astragalin	5282102	None	None	None	None
Spirostanol	12304444	None	None	None	None
Ulipristal acetate Control	130904	None	High	High	None

Fundamental Physicochemical Characteristics of Screened DS Compounds: The physicochemical properties of the identified phytochemicals, summarized in Table 3, revealed considerable structural diversity. These parameters, obtained from SwissADME, are critical indicators of pharmacokinetic behaviour and drug-likeness, influencing absorption, distribution, metabolism, and excretion.

In this study, molecular weight (MW) is a key determinant of membrane permeability and oral bioavailability, with values below 500 Da considered optimal. The compounds exhibited MW values ranging from 162.14 g/mol (7-hydroxycoumarin) to 610.52 g/mol (rutin). Heavy atom count, reflecting molecular size and complexity, varied from 12 to 43, while aromatic heavy atoms ranged from 0 (squalene, spirostanol) to 16 (quercetin, rutin, kaempferol), indicating differences in aromaticity.

Fraction of sp³ carbons reflects molecular geometry and three-dimensionality, influencing solubility and receptor interactions. This parameter ranged from 0 in fully aromatic compounds (resveratrol, quercetin) to 1.0 in the aliphatic spirostanol. Rotatable bonds, indicative of molecular flexibility and oral bioavailability, ranged from 0 (kaempferol, 7-hydroxycoumarin, spirostanol) to 15 (squalene), showing variation from rigid to highly flexible structures.

Hydrogen bond donors (HBD) and acceptors (HBA) affect solubility and permeability, forming part of Lipinski's Rule of Five. HBA values ranged from 0

(squalene) to 16 (rutin), and HBD from 0 (squalene) to 10 (rutin), suggesting substantial variation in hydrogen-bonding capacity. Topological polar surface area (TPSA), a measure of molecular polarity and hydrogen-bonding potential, influences absorption and blood-brain barrier penetration; lower TPSA values generally favor good permeability.

Molar refractivity (MR) represents molecular size and polarizability, correlating with electronic distribution and interaction potential. MR values spanned from 44.51 (7-hydroxycoumarin) to over 140 (squalene, rutin), highlighting significant differences in size and electronic characteristics.

These parameters illustrate a wide range of physicochemical behaviours among the studied phytochemicals, encompassing small, rigid aromatic molecules and large, flexible aliphatic structures.

SWISS-ADME analysis of DS phytochemicals was compared with reported profiles of *Piper longum* and *Bauhinia acuminata* (Samajdar et al., 1999; Nagamalla, et al., 2021; Jamkhedkar et al., 2023). Key parameters including molecular weight, lipophilicity (Log P), hydrogen bonding, and TPSA largely aligned with druglike ranges. Consistent with previous findings, compounds exhibiting moderate molecular weight, balanced lipophilicity, limited hydrogen bonding, and restricted flexibility are predicted to possess favorable bioavailability and pharmacokinetic properties.

Table 3. Fundamental Physicochemical Characteristics of Screened Compounds from DS Extract

	undamental l							1	
Phytochemical	Formula	Molecul	Heav	Aromati	Fractio	Rotatabl	H-bond	H-	MR
		arWeigh	У	c heavy	n Csp3	e bonds	acceptor	bond	
		t	atoms	atoms			S	donor	
								S	
3-Pentadecyl-	$C_{21}H_{36}O$	304.51	22	6	0.71	14	1	1	100.7
phenol									3
Resveratrol	C <sub>14</sub> H <sub>12</sub> O <sub>3</sub>	228.24	17	12	0	2	3	3	67.88
Dihydroguaiareti	C <sub>20</sub> H <sub>26</sub> O <sub>4</sub>	330.42	24	12	0.4	7	4	2	96.96
c Acid									
Squalene	C <sub>30</sub> H <sub>50</sub>	410.72	30	0	0.6	15	0	0	143.4
Squarene	C301130	110.72	30		0.0	13			8
Quercetin	C <sub>15</sub> H <sub>10</sub> O <sub>7</sub>	302.24	22	16	0	1	7	5	78.03
`					ŭ	_	,		
Quercitrin	$C_{21}H_{20}O_1$	448.38	32	16	0.29	3	11	7	109
	1								
Isoquercitrin	$C_{21}H_{20}O_1$	464.38	33	16	0.29	4	12	8	110.1
	2								6
Rutin	$C_{27}H_{30}O_1$	610.52	43	16	0.44	6	16	10	141.3
	6								8
Kaempferol	$C_{15}H_{10}O_6$	286.24	21	16	0	1	6	4	76.01
7-	$C_9H_6O_3$	162.14	12	10	0	0	3	1	44.51
Hydroxycoumari									
n									
Astragalin	$C_{21}H_{20}O_1$	448.38	32	16	0.29	4	11	7	108.1
	1								3
Spirostanol	$C_{27}H_{44}O_3$	416.64	30	0	1.0	0	3	1	122.0
-r	-2/			_	0		_	-	7
Ulipristal acetate	C <sub>30</sub> H <sub>37</sub> N	475.62	35	6	0.57	5	4	0	138.6
(Control)	O <sub>4</sub>	1							2
(======================================	~ 7	1	1	l	l	1	1	1	

H-bond-hydrogen bond; MR- Molar refractivity.

Lipophicility Prediction of DS Phytochemicals: Lipophilicity is a critical determinant of a compound's absorption, distribution, and membrane permeability, influencing both pharmacokinetic and pharmacodynamic behaviour. The lipophilicity of the screened phytochemicals as displayed in Table 4, expressed as consensus Log P values showed marked variation among the compounds. Squalene (9.38) and 3pentadecyl-phenol (6.89) exhibited the highest lipophilicity, indicating strong membrane affinity and poor aqueous solubility. Dihydroguaiaretic acid (4.10) displayed moderately high lipophilicity, while resveratrol (2.48), kaempferol (1.58), and quercetin (1.23) showed balanced hydrophilic-lipophilic characteristics favorable for passive diffusion and bioavailability. In contrast, quercitrin (0.16), isoquercitrin (-0.25), and rutin (-1.29)were distinctly hydrophilic, suggesting higher solubility but limited membrane permeability. Polarity, represented by the topological polar surface area (TPSA), reflects a molecule's hydrogen-bonding potential and capacity for intestinal absorption or blood-brain barrier penetration. The TPSA values ranged from 0 Å<sup>2</sup> in squalene to 269.43 Å<sup>2</sup> in rutin, demonstrating an inverse relationship with

lipophilicity. More polar compounds exhibited lower Log P values and greater hydrophilicity. The lipophilicity ranking based on consensus Log P values followed the order: squalene > 3-pentadecyl-phenol > dihydroguaiaretic acid > resveratrol > kaempferol > quercetin > quercitrin > isoquercitrin > rutin. This gradient highlights the structural diversity among the phytochemicals, influencing their predicted absorption and distribution profiles.

Previous in-silico studies on various medicinal plants with diverse phytochemical compositions have reported differing lipophilicity profiles. For instance, Ononamadu and Ibrahim (2021) found that the identified phytochemicals from *Gymnema sylvestre* and *Combretum micranthum* exhibited optimal consensus logP values which ranged between 5.01 and -6.22, indicating that most of the identified phytocompounds possess considerable lipophilic character.

Table 4: Lipophicility of the Screened DS Extract Compounds

Phytochemical	Formula	TPSA	iLog P	XLog P3	W	MLogP	Silicos-	Consensus
					LogP		IT Log P	Log P
3-Pentadecyl-phenol	$C_{21}H_{36}O$	20.23	4.77	9.92	7.03	5.54	7.2	6.89
Resveratrol	$C_{14}H_{12}O_3$	60.69	1.71	3.13	2.76	2.26	2.57	2.48
Dihydroguaiaretic Acid	$C_{20}H_{26}O_4$	58.92	3.62	4.96	4.17	3.20	4.54	4.10
Squalene	C <sub>30</sub> H <sub>50</sub>	0	6.37	11.58	10.6	7.93	10.41	9.38
Quercetin	C <sub>15</sub> H <sub>10</sub> O <sub>7</sub>	131.3 6	1.63	1.54	1.99	-0.56	1.54	1.23
Quercitrin	$C_{21}H_{20}O_{11}$	190.2 8	1.27	0.86	0.49	-1.84	0.01	0.16
Isoquercitrin	$C_{21}H_{20}O_{12}$	210.5 1	2.11	0.36	-0.54	-2.59	-0.59	-0.25
Rutin	C <sub>27</sub> H <sub>30</sub> O <sub>16</sub>	269.4 3	1.58	-0.33	-1.69	-3.89	-2.11	-1.29
Kaempferol	$C_{15}H_{10}O_6$	111.1 3	1.70	1.9	2.28	-0.03	2.03	1.58
7-Hydroxycoumarin	C <sub>9</sub> H <sub>6</sub> O <sub>3</sub>	50.44	1.44	1.58	1.50	1.04	1.97	1.51
Astragalin	$C_{21}H_{20}O_{11}$	190.2 8	0.53	0.72	-0.24	-2.10	-0.12	-0.25
Spirostanol	C <sub>27</sub> H <sub>44</sub> O <sub>3</sub>	38.69	4.42	6.49	5.79	5.08	4.30	5.22
Ulipristal acetate (Control)	C <sub>30</sub> H <sub>37</sub> NO <sub>4</sub>	63.68	3.81	3.47	5.54	3.9	5.25	4.39

TPSA-Topological Polar Surface Area; iLogP- in-house LogP (logarithm of the partition coefficient) predictor; XLogP3- extended LogP version 3; WLOGP- Wildman-Crippen LogP; MLogP- Moriguchi LogP; Silicos-IT LogP - Silicos-IT LogP predictor; Consensus LogP- Average of individual LogP predictors

Predicted Water Solubility Results of DS Extract **Phytochemicals:** The predicted solubility values for the DS phytochemicals as displayed in Table 5 varied widely among the phytochemicals, driven by polarity and structural features. 7-hydroxycoumarin showed the highest solubility. Similarly, flavonoids such as quercetin, kaempferol, astragalin, isoquercitrin, quercitrin, resveratrol and rutin showed good solubility while dihydroguaiaretic acid was predicted as moderately soluble. Lipophilic compounds such as 3-pentadecylphenol and squalene were predicted poorly soluble to insoluble. The previously reported water solubility of phytochemicals identified in Gymnema sylvestre and Combretum micranthum ranged from highly soluble to poorly soluble, consistent with the findings of this study, likely reflecting differences in molecular polarity and functional groups (Ononamadu & Ibrahim, 2021). Water solubility is a key factor in drug discovery, as it facilitates compound handling and formulation, influences absorption for orally administered drugs, and is critical

for achieving effective dosing in parenteral formulations (Daina et al., 2017).

Predicted Pharmacokinetics (ADME) of Screened DS Extract Phytochemicals: Pharmacokinetic evaluation identifies compounds with suitable absorption. distribution, metabolism, and excretion (ADME) properties essential for successful drug development. In Table 6, SwissADME analysis revealed that some compounds exhibited favourable pharmacokinetic properties, with high gastrointestinal absorption (GIA) being a common feature. Notable exceptions included 3pentadecyl-phenol, squalene, quercitrin, isoquercitrin, rutin, and astragalin, all of which showed poor oral absorption consistent with their high polarity or lipophilicity. Similar findings were reported in analyses of Bauhinia acuminata phytochemicals, where highly polar compounds exhibited limited gastrointestinal absorption (Nagamalla et al., 2021) Compounds such as resveratrol, dihydroguaiaretic acid, 7-hydroxycoumarin, and spirostanol demonstrated not only good absorption but also the ability to cross the blood-brain barrier (BBB), suggesting potential central nervous system (CNS) activity. These results align with in silico ADME predictions of Piper longum constituents, where resveratrol showed strong BBB permeability and oral bioavailability (Samajdar et al., 1999). In contrast, other

compounds with lower predicted BBB permeability are less likely to exert CNS-related effects, consistent with observations in related medicinal plants (Daina et al., 2017).

Most of the compounds are not subject to p-glycoprotein (p-gp) efflux. Only dihydroguaiaretic acid and rutin were predicted to be p-gp substrates, which may reduce their effective bioavailability (Liu & Hu, 2000).

Cytochrome P450 (CYP) interaction profiling highlighted possible drug-drug interaction risks associated with some phytochemicals of DS. Quercetin, kaempferol, and resveratrol exhibited acceptable absorption but inhibited multiple CYP isoforms. This observation aligns with previous reports showing that these flavonoids commonly inhibit CYP1A2, CYP2C9, CYP2D6, and CYP3A4, which may alter the metabolism of co-administered drugs (Gómez-Garduño et al., 2022; Showande et al., 2019). Specifically, CYP1A2 inhibition predicted for 3-pentadecyl-phenol, resveratrol, dihydroguaiaretic acid, quercetin, kaempferol, and 7hydroxycoumarin is consistent with earlier studies indicating that resveratrol and flavonoids are potent inhibitors of CYP1A2 (Rastogi et al., 2020). CYP2C19 inhibition associated with dihydroguaiaretic acid and 3-pentadecyl-phenol corroborates findings that some plant-derived compounds may modulate this isoform, impacting drug metabolism (Amaeze et al., 2021). Similarly, inhibition of CYP2D6 by kaempferol, quercetin, and dihydroguaiaretic acid concurs with documented concerns regarding flavonoid interactions with this enzyme (Showande et al., 2018).

These results suggest that compounds such as dihydroguaiaretic acid, resveratrol, quercetin, and kaempferol require caution due to significant CYP inhibition and possible drug—drug interactions. Phenolic compounds including these flavonoids have been widely reported to inhibit cytochrome P450 enzymes, which can affect drug metabolism and increase interaction risks (Galati & O'Brien, 2004). Hence, despite therapeutic potential, these compounds should be used carefully in combination therapies

Table 5. Predicted water solubility of the screened compounds

Phytochemical	ESOL Log S	ESOL Class	Ali Log	Ali Class	Silicos-	Silicos-IT
			S		IT	class
					LogSw	
3-Pentadecyl-phenol	-7.26	Poorly	-10.27	Insoluble	-7.86	Poorly
		soluble				soluble
Resveratrol	-3.62	Soluble	-4.07	Moderately soluble	-3.29	Soluble
Dihydroguaiaretic Acid	-4.92	Moderately	-5.94	Moderately	-5.67	Moderately
		soluble		soluble		soluble
Squalene	-8.69	Poorly	-11.57	Insoluble	-7.48	Poorly
-		soluble				soluble
Quercetin	-3.16	Soluble	-3.91	Soluble	-3.24	Soluble
Quercitrin	-3.33	Soluble	-4.44	Moderately	-2.08	Soluble
				soluble		
Isoquercitrin	-3.04	Soluble	-4.35	Moderately	-1.51	Soluble
				soluble		
Rutin	-3.3	Soluble	-4.87	Moderately	-0.29	Soluble
				soluble		
Kaempferol	-3.31	Soluble	-3.86	Soluble	-3.82	Soluble
7-Hydroxycoumarin	-2.46	Soluble	-2.25	Soluble	-3.03	Soluble
Astragalin	-3.18	Soluble	-4.29	Moderately	-2.1	Soluble
				soluble		
Spirostanol	-6.51	Poorly	-7.1	Poorly	-4.51	Moderately
		soluble		soluble		soluble
Ulipristal acetate (Control)	-4.77	Moderately	-4.49	Moderately	-6.77	Poorly
		soluble		soluble		soluble

ESOL Log S: Predicted Logarithm of aqueous solubility; ESOL Class: Classification of solubility based on ESOL Log S values: Ali Log S: Predicted aqueous solubility

(Log S) from the Ali et al. model; Ali Class: Solubility categories from Ali Log S predictions; Silicos-IT LogSw: Logarithm of water solubility predicted by the

JOBASR2025 3(6): 210-232

Silicos-IT FILTER-IT method: Silicos-IT Class: Solubility classification from Silicos-IT LogSw

Table 6. Predicted pharmacokinetics (ADME) parameters of the screened compounds

Phytochemical	GI absorption	BBB permeant	Pgp substrate	CYP1A2 inhibitor	CYP2C19 inhibitor	CYP2C9 inhibitor	CYP2D6 inhibitor	CYP3A4 inhibitor	log Kp (cm/s)
3-Pentadecyl- phenol	Low	No	No	Yes	Yes	No	No	No	-1.11
Resveratrol	High	Yes	No	Yes	No	Yes	No	Yes	-5.47
Dihydroguaiaretic Acid	High	Yes	Yes	Yes	Yes	No	Yes	Yes	-4.79
Squalene	Low	No	No	No	No	No	No	No	-0.58
Quercetin	High	No	No	Yes	No	No	Yes	Yes	-7.05
Quercitrin	Low	No	No	No	No	No	No	No	-8.42
Isoquercitrin	Low	No	No	No	No	No	No	No	-8.88
Rutin	Low	No	Yes	No	No	No	No	No	10.26
Kaempferol	High	No	No	Yes	No	No	Yes	Yes	-6.70
7- Hydroxycoumarin	High	Yes	No	Yes	No	No	No	No	-6.17
Astragalin	Low	No	No	No	No	No	No	No	-8.52
Spirostanol	High	Yes	No	No	No	No	No	No	-4.23
Ulipristal acetate (Control)	High	No	Yes	No	No	No	Yes	Yes	-6.74

GI absorption: Gastrointestinal absorption; BBB: Brain blood barrier; P-gp: Permease glycoprotein; CYP: Cytochrome P450; log Kp (cm/s): Skin permeability coefficient.

Predicted Drug-Likeness, Medicinal Chemistry and Lead Likeness Parameters of Diodia sarmentosa Phytochemicals: Drug-likeness analysis provides an early evaluation of whether a compound exhibits the structural and physicochemical characteristics typical of orally active drugs (Daina et al., 2017). In the present study, the consensus drug-likeness score from SwissADME, which integrates multiple rule-based filters (Lipinski, Ghose, Veber, Egan, and Muegge), was used to generate a unified and robust prediction of the drug-like potential of the screened phytochemicals (Daina et al., 2017). This consensus approach reduces bias associated with any single predictive model and offers a more reliable estimation of oral drug-likeness (Daina et al., 2017). Compounds that satisfied most or all of these rulebased criteria are considered to possess favourable oral drug-like properties (Daina et al., 2017), characterized by an optimal balance between solubility and permeability and a lower likelihood of poor pharmacokinetic performance (Daina et al., 2017). In contrast, phytochemicals violating multiple criteria mav demonstrate limited absorption, low bioavailability, or metabolic instability (Bultum et al., 2022). Nevertheless, isolated rule violations do not preclude bioactivity (Stratton et al., 2015), as several clinically approved natural-product-derived drugs deviate from one or more conventional drug-likeness thresholds (Stratton et al., 2015; Skinnider, et al., 2017). The computed druglikeness, medicinal chemistry, and lead-likeness parameters of the screened phytochemicals are summarized in Table 7. Among the compounds, resveratrol, dihydroguaiaretic acid, and kaempferol exhibited no violations across all five drug-likeness filters, suggesting high oral drug-likeness and favorable pharmacokinetic potential. All remaining compounds presented at least one violation in these filters. The bioavailability scores for most compounds were moderate (0.55), indicating a 55% probability of adequate oral absorption. However, glycosylated flavonoids such as quercitrin, isoquercitrin, rutin, and astragalin displayed significantly lower scores (0.17), reflecting their high polarity and reduced membrane permeability (Daina et al., 2017).

All compounds, with respect to lead-likeness, exhibited at least one violation, suggesting a need for further structural optimization to enhance developability. PAINS (Pan-Assay Interference Compounds) and Brenk alerts

JOBASR2025 3(6): 210-232

were identified in several phytochemicals, highlighting potential risks of assay interference or reactive substructures that may require medicinal chemistry refinement. This is consistent with the study carried out by Ranjith and Ravikumar, (2019) on *Ipomoea mauritiana* Jacq. The synthetic accessibility scores in this study also varied considerably in agreement with the report by Ranjith and Ravikumar, (2019). Simpler structures such as 3-pentadecyl-phenol showed lower synthetic complexity compared to highly functionalized molecules like rutin and spirostanol.

These results indicate that resveratrol, dihydroguaiaretic acid, and kaempferol possess the most favourable druglikeness, lead-likeness, and medicinal chemistry characteristics among the screened phytochemicals, which is in alignment with independent studies carried out by Baur and Sinclair, 2006, Calderón-Montaño et al., 2011 and National Center for Biotechnology Information, 2025. This makes the phytochemicals promising candidates for further pharmacokinetic evaluation and lead optimization.

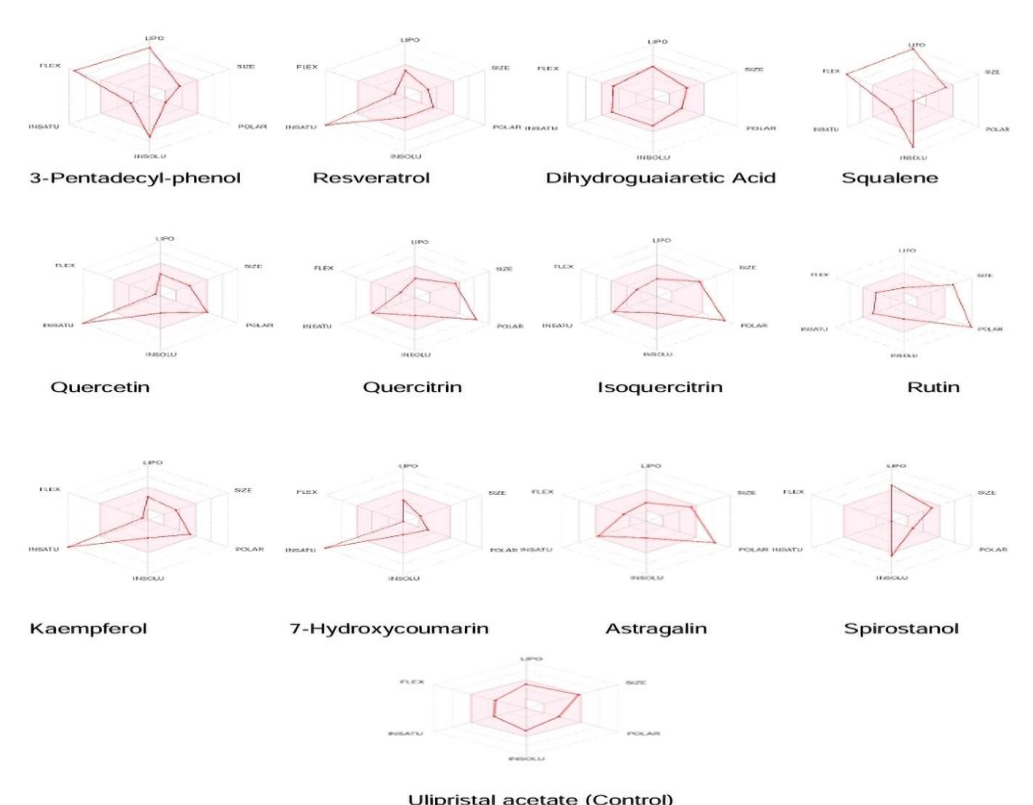
## **Bioavailability Radar Plots of DS Phytochemicals**

The bioavailability radar serves as a graphical assessment tool that complements rule-based filters by visually identifying compounds with physicochemical profiles most compatible with oral drug development (Daina et A compound whose physicochemical al., 2017). properties fall largely within this pink zone is considered to have balanced characteristics (Daina et al., 2017). In contrast, deviations outside this region indicate suboptimal properties, such as excessive lipophilicity, polarity, or molecular flexibility, which can limit absorption or distribution (Daina et al., 2017). The bioavailability radar plot predicted that dihydroguaiaretic acid had optimal drug likeness properties comparable to the control drug, ulipristal acetate among all the screened phytochemicals. Other phytochemicals such as quercetin, kaempferol and spirostanol were also selected. The rest of the phytochemicals failed to comply with the fraction of carbons in the sp3 hybridization (fraction Csp3) and water solubility criteria.

Table7: Predicted drug-likeness, medicinal chemistry and lead-likeness pharmacokinetics parameters of the screened compounds

Phytochemica	Lipins	Ghose	Veber	Egan	Muegg	Bioa	PAI	Bren	Lead	Synthetic
1 hytochemica	ki	violati	violati	violati	e	vaila	NS	k	likenes	Accessibi
•	violati	ons	ons	ons	violati	bility	alert	alert	S	lity
	ons				ons	Score	s	s	violati	
									ons	
3-Pentadecyl- phenol	1	1	1	1	2	0.55	0	0	2	2.43
Resveratrol	0	0	0	0	0	0.55	0	1	1	2.02
Dihydroguaia retic Acid	0	0	0	0	0	0.55	0	0	1	3.05
Squalene	1	3	1	1	2	0.55	0	1	3	4.73
Quercetin	0	0	0	0	0	0.55	1	1	0	3.23
Quercitrin	2	0	1	1	3	0.17	1	1	1	5.28
Isoquercitrin	2	1	1	1	3	0.17	1	1	1	5.32
Rutin	3	4	1	1	4	0.17	1	1	1	6.52
Kaempferol	0	0	0	0	0	0.55	0	0	0	3.14
7- Hydroxycoum arin	0	1	0	0	1	0.55	0	1	1	2.56
Astragalin	2	0	1	1	3	0.17	0	0	1	5.29
Spirostanol	1	2	0	0	1	0.55	0	0	2	6.88
Ulipristal acetate (Control)	0	2	0	0	0	0.55	1	0	1	5.3

PAINS: Pan-Assay interference compounds



Chipristal acctate (Control)

Fig: 3: Bioavailability Radar plot of *Diodia sarmentosa* phytochemicals

These computational models provided cost-effective and reliable alternatives to laboratory experiments (Daina et al., 2017), enabling efficient prioritization of phytochemicals through molecular docking and ADMET profiling to identify potential drug candidates.

The choice of targets used in this study is biologically and clinically justified, as uterine fibroids are hormonedependent tumours strongly influenced by estrogen and progesterone signaling (Obochi et al., 2009; Koffuor, et al. 2013 and Zia et al., 2014). Elevated ER activity has been consistently linked to fibroid growth and recurrence, supporting its selection (Borahay et al., 2017). Similarly, the progesterone receptor enhances fibroid progression by promoting cell survival and inhibiting apoptosis. Clinical use of selective progesterone receptor modulators (SPRMs), such as ulipristal acetate, highlights its therapeutic relevance (Talaulikar & Manyonda, 2013; Bestel & Donnez, 2014). The GnRH1 receptor regulates ovarian steroidogenesis through luteinizing hormone (LH) and follicle-stimulating hormone (FSH) release. Antagonists such as elagolix act on this receptor to suppress systemic estrogen and progesterone production, leading to fibroid shrinkage and symptom relief (Schlaff et al., 2020; Sánchez Martín et al., 2025).

The dual-target interactions observed among the phytochemicals suggest a potential synergistic

mechanism (Wagner & Ulrich-Merzenich, 2009) underlying the traditional use of DS in fibroid management, consistent with the multi-target nature of phytotherapeutics (Hopkins, 2008). Binding affinity alone is insufficient if compounds cannot be absorbed, distributed, or metabolized effectively. In order to ensure rational triage and identity of the most viable leads, it was essential to complement docking results with ADMET profiling and drug-likeness evaluation. Integrated docking and ADMET triage identified spirostanol as a promising in-silico candidate out of twelve hits. Spirostanol exhibited strong binding affinity, particularly toward the progesterone and GnRH1 receptors, alongside high gastrointestinal absorption. Although predicted to cross the blood-brain barrier, an undesirable trait for peripheral indications (Daina et al., 2017) its favourable molecular polarity and flexibility placed it within the drug-like zone of the bioavailability radar. This supports Veber et al. (2002), who noted that oral absorption depends more on low polar surface area and rotatable bond count than on lipophilicity. With only one Lipinski violation, spirostanol qualified as an oral candidate (Lipinski et al., 2001) and displayed mild CYP inhibition, suggesting an overall acceptable ADMET profile.

Dihydroguaiaretic acid also showed strong docking affinity, good drug likeness, bioavailability, and high GI absorption. However, its predicted BBB penetration, pglycoprotein substrate status, and inhibition of multiple CYP isoforms (CYP1A2, 2C19, 2D6, 3A4) indicate potential pharmacokinetic liabilities and a higher risk of drug-drug interactions (Daina et al., 2017), warranting structural or formulation optimization. Conversely, 3pentadecyl-phenol demonstrated moderate docking activity, low GI absorption, and poor solubility, with radar deviations in lipophilicity and solubility and a single Lipinski violation. Nonetheless, the absence of toxicity alerts suggests limited but possible scope for improvement. Flavonoids such as rutin, quercitrin, isoquercitrin, and astragalin were constrained by poor oral bioavailability, multiple Lipinski violations, and low GI absorption. Similarly, resveratrol, quercetin, kaempferol, and 7-hydroxycoumarin showed good docking scores but were flagged for potential in-silico toxicity, necessitating further safety validation.

#### CONCLUSION

This study provides the first comprehensive *in silico* assessment of phytochemicals from DS as potential modulators of hormone receptors associated with uterine fibroids. Several compounds demonstrated strong binding affinities toward at least one fibroid-related molecular target, suggesting promising therapeutic potential. These findings offer molecular-level validation for the ethnomedicinal use of DS and identify its phytochemicals as valuable scaffolds for the development of novel anti-fibroid agents. Further optimization of their ADMET properties, coupled with *in vitro* and *in vivo* validation, is recommended to enhance their pharmacological suitability and confirm biological efficacy.

## REFERENCE

Akah, P. A., Orisakwe, O. E., Gamaniel, K. S., & Shittu, A. (1998). Evaluation of Nigerian traditional medicines: II. Effects of some Nigerian folk remedies on peptic ulcer. *Journal of Ethnopharmacology*, 62(2), 123–127. <a href="https://doi.org/10.1016/S0378-8741(98)00062-2">https://doi.org/10.1016/S0378-8741(98)00062-2</a>

Amaeze, O., Eng, H., Horlbogen, L., Varma, M. V. S., & Slitt, A. (2021). Cytochrome P450 enzyme inhibition and herb-drug interaction: Potential of medicinal plant extracts used for management of diabetes in Nigeria. Biomedical and Pharmaceutical Sciences Faculty Publications. University of Rhode Island. https://digitalcommons.uri.edu/bps\_facpubs/

Anyanwu-Azuka, S. I., Aloh, G. S., Kalu, W. O., & Eleazu, C. (2022). Phytochemical screening and

evaluation of the anti-diarrhoea properties of *Diodia* sarmentosa leaves in castor oil-induced diarrhoea in albino rats. *Nutrition & Food Science*, 52(2), 255–269. https://doi.org/10.1108/NFS-03-2021-0093

Baird, D. D., Dunson, D. B., Hill, M. C., Cousins, D., & Schectman, J. M. (2003). High cumulative incidence of uterine leiomyoma in Black and White women: Ultrasound evidence. *American Journal of Obstetrics and Gynecology*, 188(1), 100–107. <a href="https://doi.org/10.1067/mob.2003.99">https://doi.org/10.1067/mob.2003.99</a>

Baur, J., Sinclair, D. Therapeutic potential of resveratrol: the in vivo evidence. *Nature Reviews Drug Discovery* 5, 493–506 (2006). https://doi.org/10.1038/nrd2060
Bestel, E., & Donnez, J. (2014). The potential of selective progesterone receptor modulators for the treatment of uterine fibroids. *Expert Review of Endocrinology & Metabolism*, 9(1), 79–92. https://doi.org/10.1586/17446651.2014.862495

Bhagavan, N. V., & Chung-Eun, H. (2011). Enzymes and enzyme regulation. In N. V. Bhagavan & C.-E. Ha (Eds.), *Essentials of medical biochemistry* (pp. 47–58). Academic Press.

Borahay, M. A., Asoglu, M. R., Mas, A., Adam, S., Kilic, G. S., & Al-Hendy, A. (2017). Estrogen receptors and signaling in fibroids: Role in pathobiology and therapeutic implications. *Reproductive Sciences*, 24(9), 1235–1244. https://doi.org/10.1177/193371911 6678686

Bultum, L. E., Tolossa, G. B., Kim, G., Kwon, O., & Lee, D. (2022). In silico activity and ADMET profiling of phytochemicals from Ethiopian indigenous aloes using pharmacophore models. *Scientific Reports*, *12*, 22221. <a href="https://doi.org/10.1038/s41598-022-26617-3">https://doi.org/10.1038/s41598-022-26617-3</a>

Calderón-Montaño, J. M., Burgos-Morón, E., Pérez-Guerrero, C., & López-Lázaro, M. (2011). A review on the pharmacology of kaempferol and its bioavailability. *Mini-Reviews in Medicinal Chemistry*, *11*(4), 298–344. <a href="https://doi.org/10.2174/138955711795305335">https://doi.org/10.2174/138955711795305335</a>

Ciceri, S., Fassi, E. M. A., Vezzoli, V., Bonomi, M., Colombo, D., Ferraboschi, P., Grazioso, G., Grisenti, P., Villa, S., Castellano, C., & Meneghetti, F. (2024). Novel non-peptide uracil-derived human gonadotropin-releasing hormone receptor antagonists. *European Journal of Medicinal Chemistry*, 279, 116903. https://doi.org/10.1016/j.ejmech.2024.116903

Daina, A., Michielin, O., & Zoete, V. (2017). SwissADME: A free web tool to evaluate pharmacokinetics, drug-likeness and medicinal chemistry

- friendliness of small molecules. *Scientific Reports*, 7, 42717. <a href="https://doi.org/10.1038/srep42717">https://doi.org/10.1038/srep42717</a>
- Dar, A. M., & Mir, S. (2017). Molecular docking: Approaches, types, applications and basic challenges. *Journal of Analytical & Bioanalytical Techniques*, 8(2), 1–3.
- De Freitas, R. F., & Schapira, M. (2017). A systematic analysis of atomic protein–ligand interactions in the PDB. *Medicinal Chemistry Communications*, 8(10), 1970–1981. https://doi.org/10.1039/C7MD00381A
- De Smit, N. S., de Lange, M. E., Boomsma, M. F., Huirne, J. A. F., & Hehenkamp, W. J. K. (2025). Current treatment for symptomatic uterine fibroids: Available evidence and therapeutic dilemmas. *The Lancet*, 406(10395), 91–102. <a href="https://doi.org/10.1016/S0140-6736(24)01857-8">https://doi.org/10.1016/S0140-6736(24)01857-8</a>
- Dourado, J. d. A. E., Lopes, S. Q., Jimenez, D. E. Q., Ramos, R. S., & Ferreira, I. M. (2025). Identification of Novel Progesterone Receptor (PR) Inhibitors (*Homo sapiens*) from Metabolites of Biotransformation Fungal: A Bioinformatics approach. *Pharmaceuticals*, 18(2), 136. <a href="https://doi.org/10.3390/ph18020136">https://doi.org/10.3390/ph18020136</a>
- Elechi, N. A., Okezie-Okoye, C., & Abo, K. A. (2020). Antidiabetic potentials of *Diodia sarmentosa* Sw. (Rubiaceae) leaves on alloxan-induced diabetic rats. *Saudi Journal of Medical and Pharmaceutical Sciences*, 6(9), 622–626. https://doi.org/10.36348/sjmps.2020.v06i09.006
- Erhirhie, E. O., & Ilodigwe, E. E. (2019). Sub-chronic toxicity evaluation of *Dryopteris filix-mas* (L.) Schott leaf extract in albino rats. *Brazilian Journal of Pharmaceutical Sciences*, 55, e18107. https://doi.org/10.1590/s2175-97902019000118107
- Ezejiofor, T. I. N., & Okoroafor, C. H. (2019). Biochemical and histopathological evidence of anticancer potentials of ethanolic leaves extract of *Diodia sarmentosa* (Sw.) against diethyl nitrosamine-induced hepatocellular carcinoma in albino rats. *Reviews in Antiviral Therapy and Infectious Diseases*, 8, 77–78.
- Ezejiofor, T. I. N., & Okoroafor, C. H. (2022). Effects of ethanol extracts of *Diodia sarmentosa* leaves on biochemical and histopathological indices of monosodium glutamate-induced uterine leiomyoma in rats. *Biomedical Research and Therapy*, 9(7), 5140–5148. <a href="https://doi.org/10.15419/bmrat.v9i7.749">https://doi.org/10.15419/bmrat.v9i7.749</a>
- Galati, G., & O'Brien, P. J. (2004). Potential toxicity of flavonoids and other dietary phenolics: significance for

- their chemopreventive and anticancer properties. *Free Radical Biology and Medicine*, 37(3), 287-303. <a href="https://doi.org/10.1016/j.freeradbiomed.2004.04.">https://doi.org/10.1016/j.freeradbiomed.2004.04.</a>
- Gómez-Garduño, J., et al. (2022). Phytochemicals that interfere with drug metabolism and transport. *Frontiers in Pharmacology, 13*, Article 870544. https://doi.org/10.3389/fphar. 2022.870544
- Hopkins, A. L. (2008). Network pharmacology: The next paradigm in drug discovery. *Nature Chemical Biology*, *4*(11), 682–690. <a href="https://doi.org/10.1038/nchembio.118">https://doi.org/10.1038/nchembio.118</a>
- Huang, J., Yuan, Y., Zhao, N., Pu, D., Tang, Q., Zhang, S., Yan, N., & Yin, H. (2021). Orthosteric-allosteric dual inhibitors of PfHT1 as selective antimalarial agents. *Proceedings of the National Academy of Sciences of the United States of America*, 118(3), e2017749118. <a href="https://doi.org/10.1073/pnas.2017749118">https://doi.org/10.1073/pnas.2017749118</a>
- Iheagwam, F. N., Ogunlana, O. O., Ogunlana, O. E., Isewon, I., & Oyelade, J. (2019). Potential anti-cancer flavonoids isolated from *Caesalpinia bonduc* young twigs and leaves: Molecular docking and *in silico* studies. *Bioinformatics and Biology Insights*, 13, 1–16. https://doi.org/10.1177/1177932219837085
- Ishikawa, H., Reierstad, S., Demura, M., Rademaker, A. W., & Kasai, T. (2009). High aromatase expression in uterine leiomyoma tissues of African-American women. *Journal of Clinical Endocrinology and Metabolism*, 94(5), 1752–1756. https://doi.org/10.1210/jc.2008-1907
- Jha, V., Bhosale, A., Kapadia, P., Bhargava, A., & Marick, A. (2023). Multitargeted molecular docking study of phytochemicals on hepatocellular carcinoma. *Journal of Applied Biology and Biotechnology, 11*(1), 116–130. https://doi.org/10.7324/JABB.2023.110117
- Kaushik, A., Kaushik, J. J., & Lal, N. (2025, August). Phytochemicals and molecular docking: A futuristic approach for drug discovery. *Trends in Pharmacology and Toxicology*, 49–55. https://doi.org/10.21124/tpt.2025.49.55
- Koffuor, A. G., Annan, K., Kyekyeku, J. O., Fiadjoe, H. K., & Enyan, E. (2013). Effect of ethanolic stem bark extract of Blighia unijugata (Sapindaceae) on monosodium glutamate-induced uterine leiomyoma in Sprague-Dawley rats. *British Journal of Pharmaceutical Research*, *3*(4), 880–896.
- Lewis, T. D., Malik, M., Britten, J., San Pablo, A. M., & Catherino, W. H. (2018). A comprehensive review of the pharmacologic management of uterine leiomyoma.

*BioMed Research International*, 2018, 2414609. https://doi.org/10.1155/2018/2414609

Li, S., Ke, S., Yang, C., Chen, J., Xiong, Y., Zheng, L., Liu, H., & Hong, L. (2022). A ligand-and-structure dual-driven deep learning method for the discovery of highly potent GnRH1R antagonist to treat uterine diseases. *arXiv preprint* arXiv:2207.11547. https://doi.org/10.48550/arXiv.2207.11547

Lipinski, C. A., Lombardo, F., Dominy, B. W., & Feeney, P. J. (2001). Experimental and computational approaches to estimate solubility and permeability in drug discovery and development settings. *Advanced Drug Delivery Reviews*, 46(1–3), 3–26. <a href="https://doi.org/10.1016/S0169-409X(00)00129-0">https://doi.org/10.1016/S0169-409X(00)00129-0</a>

Liu, Y., & Hu, M. (2000). P-glycoprotein and bioavailability: Implication of polymorphism. *Clinical Chemistry and Laboratory Medicine*, *38*(9), 877–881. <a href="https://doi.org/10.1515/CCLM.2000.127">https://doi.org/10.1515/CCLM.2000.127</a>

Mendie, L. E., & Hemalatha, S. (2022). Molecular docking of phytochemicals targeting GFRs as therapeutic sites for cancer: An *in silico* study. *Applied Biochemistry and Biotechnology, 194*(1), 215–231. https://doi.org/10.1007/s12010-021-03791-7

Mozzanega, B. (2021). Ulipristal acetate and liver injuries: While Esmya is revoked, EllaOne is allowed in repeated self-administrations possibly exceeding UPA toxic dosing with Esmya. *Journal of Hepatology*, 74(3), 750–751. https://doi.org/10.1016/j.jhep.2020.08.046

Nagamalla, S., Saketha Priya, N., Noota, D., Mudavath, P. S. J., Pachava, A., Kudumula, N., & Anuradha Bai, S. (2021). Swiss ADME properties screening of the phytochemical compounds present in Bauhinia acuminata. Journal of Pharmacognosy and Phytochemistry, 10(4), 14193. https://doi.org/10.22271/phyto.2021.v10.i4e.14193

National Center for Biotechnology Information (2025). PubChem Compound Summary for CID 11602375, (-)-Dihydroguaiaretic acid. Retrieved November 3, 2025 from

https://pubchem.ncbi.nlm.nih.gov/compound/11602375.

Noga, M., Michalska, A., & Jurowski, K. (2024). Prediction of key toxicity endpoints of AP-238, a new psychoactive substance for clinical toxicology and forensic purposes using *in silico* methods. *Scientific Reports*, *14*, 79453. <a href="https://doi.org/10.1038/s41598-024-79453-5">https://doi.org/10.1038/s41598-024-79453-5</a>

Obochi, G. O., Malu, S. P., Obi-Abang, M., Alozie, Y., & Iyam, M. A. (2009). Effect of garlic extracts on monosodium glutamate (MSG)-induced fibroid in Wistar rats. *Pakistan Journal of Nutrition*, 8(7), 970–976. https://doi.org/10.3923/pjn.2009.970.976

Okoroafor, H. C., Awagu, F. E., & Azeke, E. A. (2020). Phytochemical and antioxidant properties of *Diodia* sarmentosa Swartz leaves. *Mongolian Journal of Chemistry*, 21(47), 27–32.

Ononamadu, C. J., & Ibrahim, A. (2021). *Molecular docking and prediction of ADME/drug-likeness properties of potentially active antidiabetic compounds isolated from aqueous-methanol extracts of* Gymnema sylvestre *and* Combretum micranthum. *BioTechnologia: Journal of Biotechnology, Computational Biology and Bionanotechnology, 102*(1), 85–99. https://doi.org/10.5114/bta.2021.103765

Patil, R., Das, S., Stanley, A., Yadav, L., Sudhakar, A., & Varma, A. K. (2010). Optimized hydrophobic interactions and hydrogen bonding at the target–ligand interface leads the pathways of drug designing. *PLoS ONE*, *5*(8), e12029. <a href="https://doi.org/10.1371/journal.pone.0012029">https://doi.org/10.1371/journal.pone.0012029</a>

Rajamiriyam, M., Anchana Devi, C., Nabiya, F., & Pushpa, N. (2022). In silico analysis of plant-based bioactive compounds targeting progesterone receptors for the treatment of uterine leiomyoma. *Advances in Pharmacology and Pharmacy*, 10(4), 281–308. <a href="https://doi.org/10.13189/app.2022.100407">https://doi.org/10.13189/app.2022.100407</a>

Rama, V., Muruganantham, B., Devaki, K., & Muthusami, S. (2022). Molecular docking analysis of estrogen receptor binding phytocomponents identified from the ethyl acetate extract of Salicornia herbacea (L). *Bioinformation*, 18(3), 273–283. https://doi.org/10.6026/97320630 018273

Ranjith, D., & Ravikumar, C. (2019). SwissADME predictions of pharmacokinetics and drug-likeness properties of small molecules present in Ipomoea mauritiana Jacq. *Journal of Pharmacognosy and Phytochemistry*, 8(5), 2063–2073.

Rastogi, H., Patil, P., Sharma, G., Sharma, A., & Jana, S. (2020). Assessment of inhibition of cytochrome P450 by resveratrol through high-throughput in vitro screening: Potential herb-drug interactions. *Journal of Environment, Science and Technology*, 6(2), 58–66.

Roy, A., Kumar, P., Bisai, S., Bhowal, S., Panda, D., Jana, S., Banerjee, S., & Das, S. (2024). Molecular characterization and expression profile of estrogen

receptor subtypes in female hilsa (Tenualosa ilisha). Frontiers in Marine Science. https://doi.org/10.3389/fmars.2024.1396297

Samajdar, T., Das, S., & Sen, P. (1999). ADME prediction of phytochemicals present in Piper longum Linn. *Asian Journal of Pharmaceutical Sciences*, 4(3), 123-135.

Sánchez Martín, M. J., Huerga López, C., Cristóbal García, I., & Cristóbal Quevedo, I. (2025). Efficacy of GnRH antagonists in the treatment of uterine fibroids: A meta-analysis. *Archives of Gynecology and Obstetrics*, 311(3), 685–696. <a href="https://doi.org/10.1007/s00404-025-07932-9">https://doi.org/10.1007/s00404-025-07932-9</a>

Sani A.K., Hamza I.K., A.S., Balarabe, Nasir H.N., Kabir H. G., Lawal R. G., Kabir Z. G., Matazu H. K. and Bala M.G. (2025) Insilico Studies of Turmeric (*Curcuma Longa*) Extract. 3(4), 186-192. <a href="https://dx.doi.org/10.4314/jobasr.v3i4.21">https://dx.doi.org/10.4314/jobasr.v3i4.21</a>

Schlaff, W. D., Ackerman, R. T., Al-Hendy, A., Archer, D. F., & Barnhart, K. T. (2020). Elagolix for heavy menstrual bleeding in women with uterine fibroids. *The New England Journal of Medicine*, *382*(4), 328–340. https://doi.org/10.1056/NEJMoa1904351

Shivakumar, R., Venkatarangaiah, K., Shastri, S., Nagaraja, R. B., & Sheshagiri, A. (2018). Antibacterial property and molecular docking studies of leaf calli phytochemicals of *Bridelia scandens* Wild. *Pharmacognosy Journal*, 10(6), 1221–1229. <a href="https://doi.org/10.5530/pj.2018.6.208">https://doi.org/10.5530/pj.2018.6.208</a>

Showande, S. J., Fakeye, T. O., Kajula, M., Hokkanen, J., & Tolonen, A. (2018). Potential inhibition of major human cytochrome P450 isoenzymes by selected tropical medicinal herbs—Implication for herb—drug interactions. *Food Science & Nutrition*, 6(8), 2431–2441. <a href="https://doi.org/10.1002/fsn3.789">https://doi.org/10.1002/fsn3.789</a>

Skinnider, M. A., Dejong, C. A., Franczak, B. C., McNicholas, P. D., & Magarvey, N. A. (2017). Comparative analysis of chemical similarity methods for modular natural products with a hypothetical structure

enumeration algorithm. *Journal of Cheminformatics*, 9, 46. <a href="https://doi.org/10.1186/s13321-017-0234-y">https://doi.org/10.1186/s13321-017-0234-y</a>

Stratton, C. F., Newman, D. J., & Tan, D. S. (2015). Cheminformatic comparison of approved drugs from natural product versus synthetic origins. Bioorganic & Medicinal Chemistry Letters, 25(21), 4802–4807. <a href="https://doi.org/10.1016/j.bmcl.2015.07.014">https://doi.org/10.1016/j.bmcl.2015.07.014</a>

Talaulikar, V. S., & Manyonda, I. (2013). Progesterone and progesterone receptor modulators in the management of symptomatic uterine fibroids. *European Journal of Obstetrics & Gynecology and Reproductive Biology*, 167(1), 1–8. <a href="https://doi.org/10.1016/j.ejogrb.2012.10.013">https://doi.org/10.1016/j.ejogrb.2012.10.013</a>

Umoh, U. F., Ajibesin, K. K., & Ubak, N. G. (2016). Preliminary anti-inflammatory and analgesic effects of *Diodia sarmentosa* Sw. leaf in rodents. *World Journal of Pharmacy and Pharmaceutical Sciences*, 5(9), 203–212.

Veber, D. F., Johnson, S. R., Cheng, H. Y., Smith, B. R., & Ward, K. W. (2002). Molecular properties that influence the oral bioavailability of drug candidates. *Journal of Medicinal Chemistry*, 45(12), 2615–2623. <a href="https://doi.org/10.1021/jm020017n">https://doi.org/10.1021/jm020017n</a>

Wagner, H., & Ulrich-Merzenich, G. (2009). Synergy research: Approaching a new generation of phytopharmaceuticals. *Phytomedicine*, *16*(2–3), 97–110. https://doi.org/10.1016/j.phymed.2008. 12.018

Zhang, Z., Huang, H., Jiang, K., Liu, W., Xuan, Y., & Lu, W. (2025). Global, regional, and national uterine fibroid burdens from 1990 to 2021 and projections until 2050: Results from the GBD study. *BMC Women's Health*, 25, 423. <a href="https://doi.org/10.1186/s12905-025-03974-y">https://doi.org/10.1186/s12905-025-03974-y</a>

Zia, M. S., Qamar, K., Hanif, R., & Khalil, M. (2014). Effect of monosodium glutamate on the serum estrogen and progesterone levels in female rats and prevention of this effect with diltiazem. *Journal of Ayub Medical College, Abbottabad, 26*(1), 18–20.